Original Article

Performance characteristics of a conformal ultra-wideband multilayer applicator (CUMLA) for hyperthermia in veterinary patients: a pilot evaluation of its use in the adjuvant treatment of non-resectable tumours

O. A. Smrkovski[1], Y. Koo[2], R. Kazemi[2], L. M. Lembcke[1], A. Fathy[2], Q. Liu[2], and J. C. Phillips[1]

[1]Department of Small Animal Clinical Sciences, The University of Tennessee, C247 Veterinary Teaching Hospital, Knoxville, TN 37996-4554, USA
[2]Department of Electrical Engineering and Computer Science, The University of Tennessee, Knoxville, TN, USA

Abstract

Performance and clinical characteristics of a novel hyperthermia antenna operating at 434 MHz were evaluated for the adjuvant treatment of locally advanced superficial tumours in cats, dogs and horses. Electromagnetic simulations were performed to determine electric field characteristics and compared to simulations for a flat microwave antenna with similar dimensions. Simulation results show a reduced skin surface and backfield irradiation and improved directional irradiation (at broadside) compared to a flat antenna. Radiated power and penetration is notably increased with a penetration depth of 4.59 cm compared to 2.74 cm for the flat antenna. Clinical use of the antenna was then evaluated in six animals with locoregionally advanced solid tumours receiving adjuvant chemotherapy. During clinical applications, therapeutic temperatures were achieved at depths ≥ 4 cm. Objective responses were seen in all patients; tissue toxicity in one case limited further therapy. This antenna provides compact, efficient, focused and deep-penetrating clinical hyperthermia for the treatment of solid tumours in veterinary patients.

Correspondence address:
J.C. Phillips
Director of Research
College of Veterinary and
Comparative Medicine
Lincoln Memorial University
Harrogate, TN 37752
email: jphill35@me.com

Introduction

Multiple generations of microwave antennae have been developed for the application of superficial hyperthermia in the treatment of solid tumours. Traditionally, these antennae can be grouped into waveguide applicators and the more compact flat or sheet applicators.[1] Waveguide applicators are physically bulky, difficult to use on contoured anatomic sites, inefficient and have a large normal electric field component, which can lead to treatment-limiting hot spots at tissue interfaces.[1–5] Furthermore, the application of water boluses are required to limit the near field effects and improve the physical coupling of the antenna to the patient; although tissue matching properties, effective field size (EFS) and effective heating depth (EHD) remain generally poor.[1,5] Flat microwave antennae offer a variety of technical improvements over waveguide applicators, including conformability, reduced size and weight, low manufacturing cost and overall improved efficiency.[5–8] Although many flat antennae designs

have been described, perhaps the most common are microstrip-based antennae formulated using printed circuit boards (PCB).[5–8] PCB can be manufactured at low cost and the substrate can be chosen to be flexible. The conformability of a flexible antenna leads to improved contact between applicator and contoured anatomic sites (e.g. extremities). Multi-element antenna arrays can also be created which allows for improved power deposition patterns, increased field size and more uniform heating.[5–8] While antenna efficiency, tissue matching properties and EFS can be significantly improved using these flat antennae, the dominance of the near-field component still requires the use of a water bolus and generally limits the heating capabilities of these devices for the treatment of superficial tumours.[2,9]

There are several approaches that can be used to reduce the near-field component and improve the overall efficiency of flat microstrip-based antennae, while maintaining their desirable conformability. The use of a slot-antenna and microstrip feedline improves bandwidth (i.e. tissue matching properties), EFS and overall efficiency; however, the bidirectional irradiation of slot antennae may lead to safety concerns. The addition of multiple layers to the flat antenna construct allows for the addition of a floating ground plane and additional slots; thus improving directionality and efficiency, respectively.[5–7,10] Manipulation of the size and shape of individual slots can lead to reductions in antenna size and changes in resonant frequency.[5,10] The addition of metamaterial-inspired periodic structures can further reduce antenna size and improve efficiency.[11–14] Finally, by using high impedance substrates for the individual layers of a multilayer antenna, unwanted surface waves can be reduced and antenna efficiency increased further.[14] The novel antennae thus created can be utilized to address the near-field components associated with the delivery of electromagnetic radiation to biologic tissues; including, unwanted surface waves, poor energy distribution across inhomogeneous boundaries, inadequate depth of penetration and low antenna efficiency.[15,16] Applicators or antennas that take advantage of these modifications may prove

quite useful in providing superficial hyperthermia treatments.

Superficial hyperthermia for the treatment of tumours generally involves raising tumour tissue temperature above 42°C for a sufficient period of time to allow for tumour tissue damage, while sparing normal tissue.[16] As a single modality, superficial hyperthermia has not been thoroughly evaluated in veterinary medicine; rather it has been described in various combinations with either radiation therapy or chemotherapy.[8,17–19] Strong biologic rationale supports the use of hyperthermia in these combination protocols because of the synergism seen with these modalities.[20,21] For example, platinum-based (Pt) chemotherapeutics are commonly used to treat solid tumours; however, resistance generally limits their use to the adjuvant setting in patients with minimal residual disease.[21–23] Although the mechanisms for resistance are multifactoral, methods that can enhance the effects of platinum-based drugs should improve response and lengthen the progression-free interval in treated patients. Hyperthermia has been shown to enhance the effect of platinum-based drugs by increasing their accumulation within tumours and the rate of Pt-DNA adduct formation.[20–23] Results seen with such combination protocols in both human and veterinary medicine demonstrate improved objective response rates and control intervals.[19,21–23]

While definitive improvements in outcome have been shown using these combination radio- or chemo-thermotherapy combinations, the hyperthermia antennae used remain relatively inefficient and can be difficult to use.[1,8,19,21–24] Here, we describe a novel antenna that is easy to use, efficient and capable of delivering an improved thermal dose to superficial inhomogeneous tissues. This technology uses a multilayer construct, which incorporates a microstrip feedline, slot-aperture antenna, periodic-resonant structures and high impedance substrates to achieve a conformal ultra-wideband multilayer applicator (CUMLA). Simulation data is used to illustrate the improved near field electric field distribution and efficiency of the CUMLA as compared to a similar dimension flat microwave antenna. We further demonstrate, in a pilot study, the safety and clinical use of the CUMLA in patients receiving carboplatin chemotherapy. Outcome is

then compared to prior reports of combination chemo-thermotherapy protocols.[19,20,23] The results of this study provide evidence of the CUMLA's ease of use and ability to deliver clinically relevant hyperthermia.

Materials and methods

Microwave hyperthermia device

Hyperthermia was delivered using a flexible multilayer antenna construct as shown in Fig. 1. This multi-layer construct is composed of various layers of flexible silicone (i.e. high impedance) substrate that separate the two PCB. All layers with printed patterns are flexible to allow for conformal application to variety of anatomic sites. A thermosensor is incorporated into the antenna

to allow for treatment monitoring and control. The antenna is powered by a microwave transceiver operating at 434 MHz with a variable power output of 5–25 W. Treatment time and surface temperature are input by the user through a control board interface. Power output is then controlled automatically through feedback from the antenna thermosensor, with maximal power during initial tissue heating and reducing to near zero at or above target temperature. In addition to this classic on–off control, output can be further modified by altering pulse repetition and/or pulse width based on feedback from the thermosensor to the control unit. During initial heating, the interval can be shortened and/or the pulse width can be increased to speed up acquisition of a pre-set target temperature. At target temperature, these values
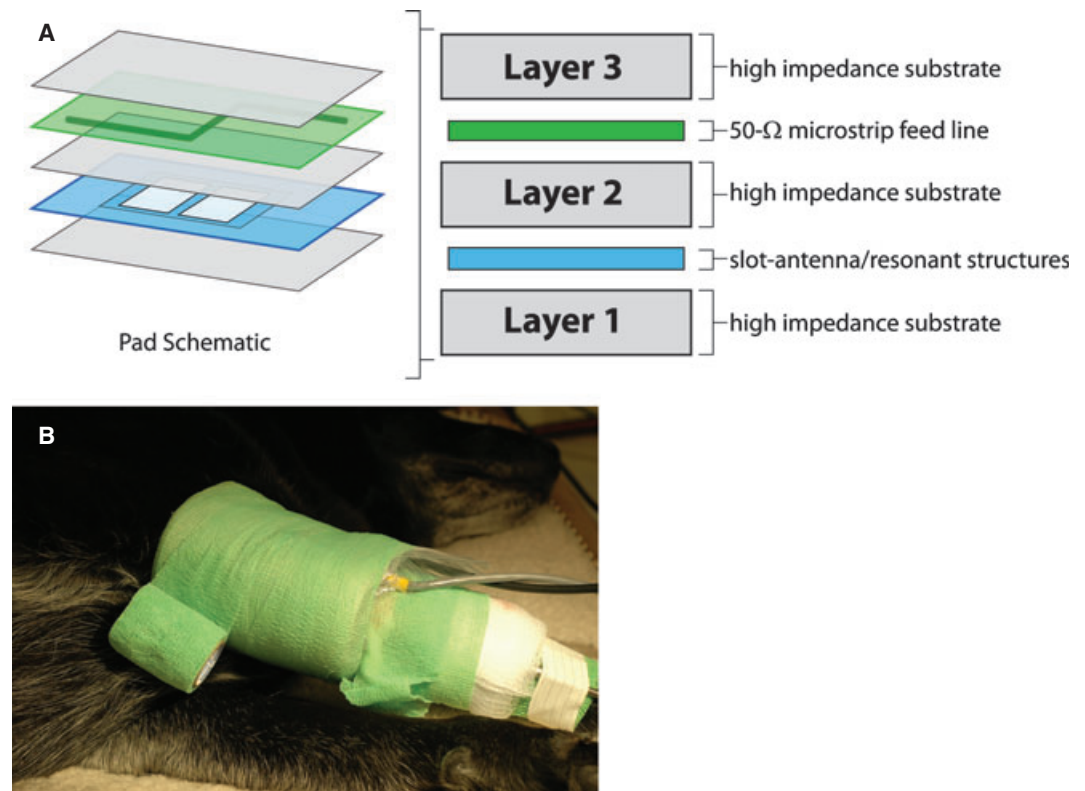

Figure 1. Antenna schematics and clinical use. (A) Schematic side view of the $11 \times 15 \times 1.5$ cm multilayer antenna construct used in this study (not to scale). The slot-antenna with periodically loaded resonant structures (blue) is separated from the 50-Ω microstrip feed line (green) by high impedance substrate (layer 2). The effective radiating aperature of the slot-antenna measures 35.9 cm^2. Additional layers of high impedance substrate are placed below the slot-antenna and above the microstrip feed line (layers 1 and 3). The floating shield plane can be placed above layer 3 (not shown). (B) Clinical application of the multilayer antenna to the elbow region of dog 2. The antenna is conformed tightly to the elbow region using elastic wraps. Temperature and coaxial control cables can be seen exiting the wraps.

can then be adjusted to maintain constant surface temperatures.

Electric field simulations

Electric field simulations were performed using the *CST Studio Suite*™ 2010 software (CST Computer Simulation Technology AG, Framingham, MA, USA) and uses the finite integration technique to generate three-dimensional (3D) full-wave field simulations.[25] This technique describes the electric field throughout a given volume subject to a set of boundary conditions and allows for direct solution of electromagnetic fields without surrounding the solution domain by an air volume.[25] Software input parameters include frequency, power, applicator structure (dimensions, material, etc) and 3D boundary conditions to include all tissues in contact with the applicator. Output parameters include electrical field solutions along with estimation of specific absorption rates (SAR). SAR provides estimates of the total real power that is transmitted into the tissues. For comparison, a simple flat microwave antenna fed by a 50-Ω microstrip line was also simulated. This flat antenna includes the same microstrip feedline used in the multi-layer construct without any further modifications. Tissue composition was assumed to be equivalent to a single-layer muscle tissue with a permittivity of $\varepsilon = 56$ and conductivity of $\sigma = 0.8$ S/m.[26] Microwave generator output power for both the CUMLA and comparative antenna was assumed to be 25 W; equivalent to 44 dB. All simulations were performed on an *Intel*® *Core*™ i7 2.67 GHZ PC with 12 GB RAM running *Windows XP* 64 bit operating system. Computation time for each simulation varied from 3 to 5 h.

Bandwidth measurement (S_{11} parameter)

The S_{11} parameter measures the reflection of energy as a result of mismatch between applicator and tissue impedance expressed in terms of input return loss (dB). Measurements were performed using an Agilent E8386B Network Analyzer (Agilent Technologies; Santa Clara, CA, USA) connected to the CUMLA in a typical single port setup in three different species; a dog, a cat and a horse. These properties are useful in determining the efficiency of energy transfer for different antenna locations and configurations. All measurements were made while holding the applicator (antenna) in contact with numerous anatomic locations in each species, including: extremities, ventral and lateral abdomen, ventral and lateral thorax, cervical, periorbital, nasal, inguinal and gluteal regions. Return loss was measured in decibels (dB) as a function of wavelength extending from 10 MHz through the frequency centre of 434 MHz, up to 2 GHz. Acceptable tissue matching between tissue and applicator was defined as a return loss < -10 dB.[27] Bandwidth was determined at a centre frequency of 434 MHz.

Clinical application of the CUMLA

Animals

A prospective pilot study to evaluate thermal characteristics and clinical use of the CUMLA was conducted in six client-owned animals (two cats, two dogs and two horses) receiving carboplatin chemotherapy. All patients were treated at the College of Veterinary Medicine, University of Tennessee. Multiple tumour types and species were selected to assess the broad applicability of the CUMLA. Patients selected for treatment with the CUMLA included those with locally advanced superficial sarcomas or carcinomas who were not candidates for, or who had failed, surgical resection. Additional enrolment criteria included a pre-treatment diagnosis, tumour measurements between 2 and 15 cm in the longest dimension, superficial tumour location (i.e. where heating was technically feasible), anticipated life expectancy of at least 4 weeks and informed owner consent. Patients with both naïve and recurrent disease were eligible for enrolment. Exclusion criteria included significant co-morbid illness that precluded chemotherapy and/or hyperthermia, radiation and/or chemotherapy (including NSAIDs) within 3 weeks before starting the protocol, round cell tumours (i.e. mast cell and lymphoma), no measureable disease and tumours deemed 'unheatable'. A tumour was deemed 'unheatable' if a minimum of 2 CEM43°C could not be achieved during a 60-min treatment period.[8,17,18] Tumour staging was carried

out by use of a modified tumour/node/metastasis classification system.[28] The following information was documented before treatment: signalment, weight, longest tumour diameter, digital images, previous treatments (i.e. surgery, radiation therapy and chemotherapy) and concurrent medications. Additional staging diagnostics included a CBC, chemistry panel with electrolytes, urinalysis, thoracic radiographs, abdominal radiographs and ultrasound when indicated. In patients with multiple tumour sites, a single target lesion was identified for treatment and evaluation of response. All evaluations were performed under the direct supervision of a board certified veterinary oncologist.

Chemotherapy administration

All enrolled patients were scheduled to receive either intralesional or systemic carboplatin. Carboplatin chemotherapy was selected based on tumour histology, previous literature describing the combination of platinum drugs and hyperthermia and the safety profile of this particular drug in both dogs and cats.[29,30] Chemotherapy treatments were administered every 3 weeks, immediately before hyperthermia treatments. Patients with tumours lacking obvious bone involvement were treated intralesionally, while patients with bone involvement received systemic chemotherapy. In horses, carboplatin was injected intralesionally at a dosage of 10 mg cm^{-3} (i.e. 1 ml drug cm^{-3}) of tumour tissue, as previously reported.[19,31] In dogs and cats, body surface area was used to calculate dosages of 275 and 225 mg m^{-2}, respectively. Patients with biochemical evidence of renal insufficiency received a minimal dosage reduction of 25%. These dose levels were established through clinical use at UTCVM and are slightly lower than those reported previously in dose escalation studies in dogs and cats.[32,33] In an attempt to achieve uniform distribution of chemotherapy in these patients, the dosage was delivered in a parallel-row fashion with multiple planes used for larger tumours.[19,31] Additives such as oil or epinephrine were not included. All systemic dosages of chemotherapy were diluted in 25−50 ml of 5% dextrose and given through peripheral intravenous catheters over 20 min.

Hyperthermia treatments and response determination

Hyperthermia treatments were applied by placing the CUMLA such that the tumour was centred on the applicator pad. No specific shielding of the eye was deemed necessary for periorbital tumours. Once an appropriate site/orientation of the antenna was selected, the applicator pad was then conformed closely to the specific anatomic location and secured in place with bandaging tape when necessary. Local anaesthetic (2% lidocaine) was utilized to facilitate invasive thermocouple placement and for intralesional chemotherapy (see below). General anaesthesia was not required, patients were held with minimal restraint during treatments. Where necessary to facilitate both restraint and treatments, sedation was provided using acepromazine (0.02−0.05 mg kg^{-1} IV) and butorphanol (0.1−0.4 mg kg^{-1} IV) in small animals or detomidine (3−5 μg kg^{-1} IV) in equine patients. Temperature was monitored using non-invasive surface measurements in all patients. In two patients, additional invasive (intra-tumoural) temperature measurements were recorded along the path of catheters placed within the tumour. The catheters were positioned perpendicular to the electric field direction at a depth of 4 cm within the tumour. The tip of the catheter was placed in line with the centre of the radiating aperture. Catheter location was determined visually and confirmed with ultrasound. Digital readouts from both invasive and non-invasive (surface) thermoprobes were continuously monitored during treatments. Average temperatures over consecutive 5-min period were used for thermal dose calculations. Owing to patient constraints, the number and location of temperature probes were chosen to be near the theoretical maximum (SAR = 100%) and minimum (SAR = 13.5%) SAR as defined by simulation studies.[34]

Treatment temperatures in all patients were set for a maximal surface temperature (T_{max}) of 41°C and/or a maximal intra-tumoural temperature of 47°C, based on estimated tissue tolerance.[35] These temperatures were maintained automatically by varying power output, pulse width and/or pulse repetition interval as a function of surface temperature. Parameters recorded included time to

reach a surface temperature $\geq 39°C$, T_{max}, average treatment temperature (T) and treatment duration (both individual and cumulative). The time–temperature curve for each thermocouple (surface and invasive) was converted to an equivalent number of minutes exposure to $43°C$ using the method of Sapareto,[36] with the following equation:

$$CEM43°C = (\Delta t)R^{(43-T)} \quad (1)$$

where Δt is 5 min, T is average measured temperature over each 5-min time period and $R = 0.25$ when $T < 43.0°C$ and 0.5 when $T > 43°C$. On the basis of this equation, temperatures below $39°C$ were not assumed to contribute significantly to the thermal dose.[17] All patients were scheduled to receive a high cumulative thermal dose (20–50 CEM43°C) as determined using non-invasive surface measurements. The targeted high cumulative thermal dose was selected based on the safety and activity seen in previous reports.[17–20] Where applicable, cumulative thermal dose was also calculated using invasive thermal measurements; although these were not used to determine prescribed dose. For uniformity, the scheduled thermal dose was delivered over a 4-week treatment period with individual hyperthermia treatments (1–3 times weekly) further constrained to last a maximum of 60 min. The total number of hyperthermia treatments varied between patients depending on the rate of heat acquisition and presence of tissue toxicity. Because of this variation, the actual number of heat treatments delivered and the cumulative CEM43°C was documented in all patients. After completion of the initial 4-week treatment regimen, additional therapy was allowed pending response and clinician assessment.

End points of interest included objective tumour response, local tissue toxicity and survival. While patients were assessed before each treatment during the protocol, objective response determinations were performed 4-week post-treatment completion to allow for resolution of the acute side effects. Additional response evaluations were performed monthly post-treatment completion until progressive disease was noted. Objective tumour response was based on the comparison of pre- and post-treatment measurements of target lesions and evaluated using modified RECIST criteria.[37] A complete response was defined as the disappearance of the target lesion. Partial response was defined as a minimum of 30% decrease in the longest dimension of the target. Progressive disease was defined as a minimal increase of 20% in the longest diameter of the target lesion. Stable disease included target lesions with neither sufficient shrinkage to qualify as a partial response nor sufficient increase to qualify for progressive disease. No additional treatments were performed in patients with either a complete response or progressive disease as defined 4-week post-treatment completion. For compassionate use, patients with partial response or stable disease were eligible for continued treatments (~2 CEM43°C/treatment) until either a complete response or progressive disease was noted at which point therapy was stopped. While targeted thermal dose prescription (i.e. 20–50 CEM43°C per month) remained constant in patients receiving compassionate use therapy, the total number of treatments varied depending on the rate of thermal dose acquisition. These additional treatments were not included in determining initial objective response rates. Toxicity was graded using the Veterinary Co-operative Oncology Group–Common Terminology for Adverse Events (VCOG–CTCAE) v1.0 descriptive terminology.[38] Haematologic toxicity was monitored through weekly complete blood-counts. Similar to previous reports, local skin and soft tissue/muscle toxicity was determined before each treatment and at re-evaluation; therapy was stopped if extensive tumour necrosis, excessive tissue sloughing, or grade III or higher toxicity was observed.[17–20] Progression-free survival was defined as the time from the date of the first hyperthermia treatment until local tumour progression or metastasis. Overall survival was defined as the time from the date of the first hyperthermia treatment until death from any cause.

Results

Electrical field simulations and comparison to a flat antenna

Simulation results for specified input settings were computed separately for each applicator type using common boundary conditions. Two-dimensional (2D) near electrical field (E-field) simulation results

are illustrated in Fig. 2 for an antenna centred at $(x, y, z) = (0, 0, 0)$. These near field simulations provide information on electric field directivity and distribution. In the x, z-plane (left images), the bottom field represents the forward radiated field (towards tissue), while the top represents the backfield irradiation. The 11×15 cm CUMLA device appears to have a favourable electric field distribution. Specifically, the electric field for the CUMLA is relatively uniform across the length of
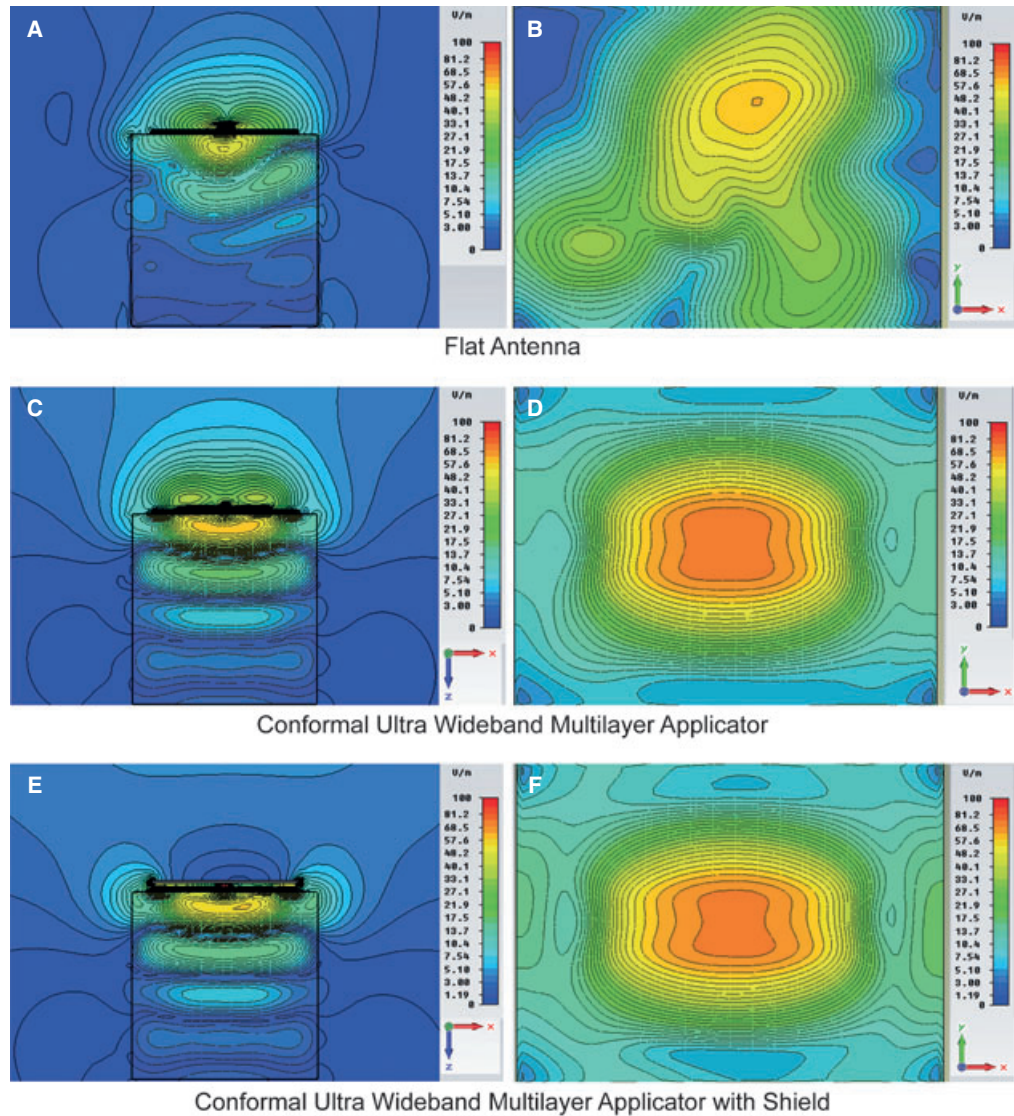

Figure 2. Two-dimensional near E-field simulation results for the antenna centred at $(x, y, z) = (0,0,0)$. Relative electric field intensity (V/m) is shown in each figure. Colours show field intensity and are similarly scaled for comparative images. Simulations were performed using *CST Studio Software* and a single-layer boundary condition ($\varepsilon = 56; \sigma = 0.8$ S/m). (A) Near field representation for a simple flat antenna in the x, z-axis. Note the high surface component and lack of field directivity. (B) Near field representation for the flat antenna taken at 1-cm depth in the x, y-axis. Note the relatively small field dimensions. (C) Near field representation for the CUMLA in the (x, z)-axis. Note directivity, depth of penetration and the relative skin sparing effective. (D) Near field representation for the CUMLA taken at 1-cm depth in the x, y-axis. Note the relatively large field dimensions. (E) Near field representation for the CUMLA in the (x, z)-axis with the addition of a floating shield plane. Note the improved directivity and elimination of backfield irradiation. (F) Near field representation for the CUMLA at 1-cm depth in the x, y-axis with the addition of a floating shield plane. No significant change in field size is noted with addition of shield plane.

the antenna and penetrates deep within the soft tissue boundary, while exhibiting a sparing effect of the skin surface. Although backfield irradiation is present, it is much lower in intensity than the main field. The addition of a floating shield plane eliminates the backfield irradiation with no significant effect on antenna efficiency. The comparative electric field generated by a simple flat antenna is shown at the top and has a maximum intensity at the surface boundary; exhibiting no skin sparing effect. Furthermore, no appreciable directivity is seen with the electric field radiated in 2D around the simple flat antenna; resulting in high electric field for both forward field and backfield.

To compare the relative size of the electrical fields generated with each antenna, near field representations for both constructs in the *x*, *y*-plane at 1-cm depth are shown in Fig. 2. The contoured electric field size of the CUMLA is 258% larger (75 versus 29 cm^2) in the (x, y)-plane in comparison to that generated by the flat antenna at similar field intensity (50% SAR). Near field simulations were also used to calculate SAR for each of the different antennas (Fig. 3). Values are typically compared at a point called the skin depth, defined as the depth into tissues (*z*-axis) at which only 13.5% (SAR = 13.5% or $1/e^2$) of the total absorbed dose remains. Using this terminology, the CUMLA has a skin penetration depth of 4.59 cm, while the flat antenna has a skin depth of 2.74 cm.

On the basis of these differences in skin depth, the CUMLA is able to penetrate approximately 68% deeper than a comparable flat antenna, while at the same time achieving a more favourable electric field distribution.

Bandwidth measurement (S_{11} parameter)

Bandwidth measurements for various anatomic locations in each species are presented in Table 1. Tissue matching properties were excellent (−10 dB for >260 MHz bandwidth) at all anatomic sites in each species with the exception of extremity locations in the cat where it was difficult to appropriately conform the antenna to the tissue (−10 dB for 40 MHz bandwidth). Representative return loss values (dB) are plotted as a function of frequency in Fig. 4.

Clinical application of the CUMLA

To evaluate the clinical use of this multilayer antenna, six companion animals were enrolled in a combination chemotherapy and hyperthermia protocol. Descriptive characteristics of each patient are listed in Table 2. Prior therapies included surgery (1), radiation therapy (1), cryotherapy (1) and chemotherapy (3). One dog had previously failed a combination of carboplatin chemotherapy and radiation therapy immediately before initiating this protocol (dog 1). One cat developed locally
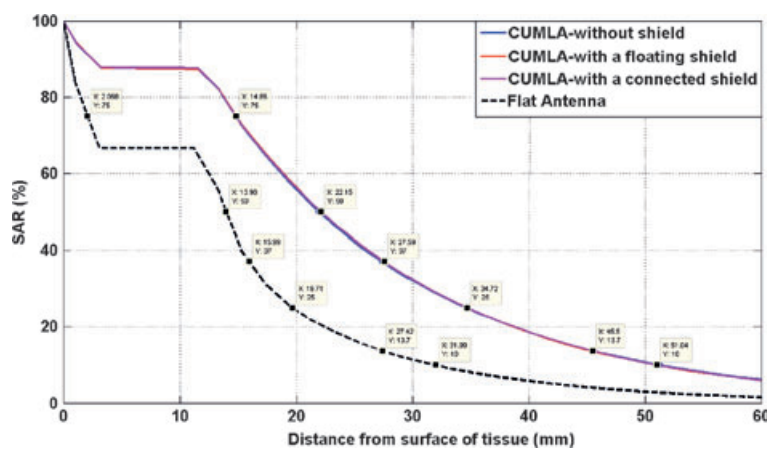

Figure 3. Comparison of specific absorption rates as a measure of the real power transmitted to the tissue boundary. The CUMLA (blue) has a significantly improved penetration depth (SAR$_{13.7\%}$ = 4.6 cm) compared to a flat antenna (dotted line) with similar dimensions (SAR$_{13.7\%}$ = 2.7 cm). The addition of a shield plane to the CUMLA (pink/red) has no significant effect on SAR (SAR$_{13.7\%}$ = 4.6 cm). All simulations were performed using *CST Studio Software*.

Table 1. Bandwidth measurements (GHz) for various anatomic locations in the horse, dog and cat

	Bandwidth (MHz)		
Anatomic site	**Horse**	**Dog**	**Cat**
Gluteal	400	350	400
Epaxial	380	340	340
Pectoral	450	360	—
Shoulder	420	360	—
Abdomen	410	380	370
Tumour	430	270	350
Extremity (flat)	380	360	<50
Extremity (curved)	270	260	0

Bandwidth measurements were determined at a frequency centre of 434 MHz with acceptable return loss defined as <-10 dB. Tumour measurements were performed on horse 1, dog 2 and cat 1, respectively. Bending the applicator to conform to a limb resulted in degraded bandwidth (and S_{11} parameters) for all extremity locations.

recurrent disease following an aggressive surgical resection (cat 1). Both horses had previously failed surgical resections and intralesional chemotherapy (5-fluorouracil). The remaining cat and dog had locally advanced tumours and were not considered candidates for primary surgical resection. Tumours were considered stage 3 or higher except for one patient who was diagnosed with multiple stage 2

tumours (cat). Tumour types included melanoma, squamous cell carcinoma and sarcoma. Tumour locations included facial (2), extremity (2) and trunk (2). Tumour volumes ranged from 2.0 to 270 cm^3 (mean 110.3 cm^3, median 97.5 cm^3). Follow up on all patients was in excess of 310 days; one patient died secondary to local tumour progression, another patient died from concurrent illness, while the remaining four patients were alive at the end of this study. Five patients completed the initially planned treatment protocol while one patient failed to receive the prescribed cumulative thermal dose because of early complete tumour necrosis (horse 1).

Specifics of thermochemotherapy treatments, response and toxicity are presented in Table 3. Thermal measurements from a typical hyperthermia treatment are illustrated in Fig. 5. Hyperthermia treatments varied from 8 to 12 per patient with a median total cumulative thermal dose (CEM43°C) of 32.7 min in the five patients who received the prescribed thermal dose. The remaining patient (horse 1) stopped after a single hyperthermia treatment (CEM43°C = 3.2 min) because of acute tumour necrosis. Invasive thermal measurements were performed in two patients; thermal
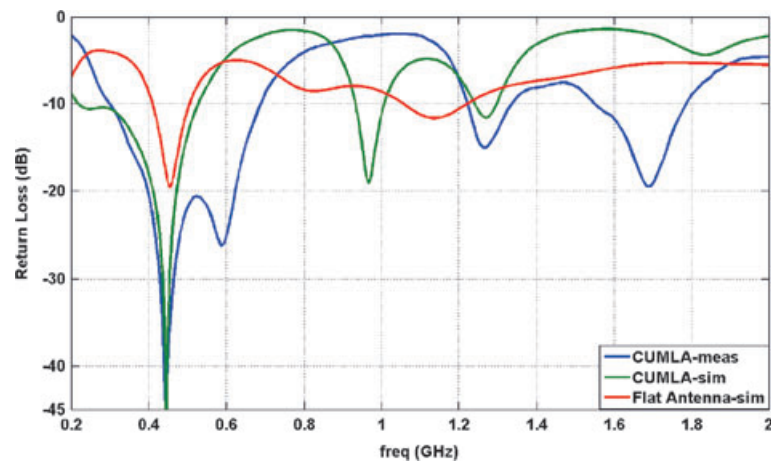

Figure 4. Measured and simulated return loss (dB) values as a function of frequency (GHz). Measured values were determined using an Agilent E8386B Network Analyzer, while simulations were performed using *CST Studio Software*. Lower return loss (dB) suggests improved energy transfer and thus tissue matching properties, at a given frequency. On the basis of the simple logarithmic scale, a decrease in return loss from −10 dB to −20 dB corresponds to an increase in energy transmission from 90 to 99%. Simulated values for the CUMLA are shown in green while measured values taken while holding the antenna on the gluteals of a horse are shown in blue. Values for a simple flat antenna are shown in red. Measured (blue) and simulated (green) values are quite comparable and exhibit similar broadband behaviour over the centre frequency; variation between the values are likely attributable to differences in boundary conditions. Bandwidth measurements (<−10 dB) were taken at a frequency centre of 434 MHz and are presented in Table 1.

Table 2.   Signalment, tumour type, clinical stage, prior treatments, for six animals treated with carboplatin and hyperthermia

Patients	Signalment	Tumour type	Previous treatment	Location	Stage
Horse 1	21-year-old M Paso Fino	Melanoma	5-FU	Ventral tail	T4N0M0
Horse 2	20-year-old F Paint	SCC	CT, 5-FU	Periocular	T3N0M0
Dog 1	6-year-old SF Mix	OSA	RT, Carbo, Doxo	Maxilla	T3bN0M0
Dog 2	9-year-old MN Labrador	HPA	None	Elbow	T3N0M0
Cat 1	15-year-old MN DSH	FSA	Surgery	Flank	T2(2)N0M0
Cat 2	6-year-old SF DSH	FSA	None	Flank	T3N0M0

5-FU, 5-Fluorouracil; Carbo, carboplatin; CT, cryotherapy; Doxo, doxorubicin; FSA, fibrosarcoma; HPA, haemangiopericytoma; OSA, osteosarcoma; SCC, squamous cell carcinoma; RT, radiation therapy.

Table 3.   Treatment parameters, tumour response and toxicity in six animals treated with carboplatin and hyperthermia

Patients	Carboplatin dosage (#treatments)	Hyperthermia treatments	CEM43°C$_S$ (CEM43°C$_I$)	Tumour response	Toxicity grade	Progression-free survival (days)	Overall survival (days)
Horse 1	800 mg IL (1)	1	3.2 (160)	CR	4[a]	430	430
Horse 2	40 mg IL (2)	8	23.1	CR	2	>500	>500
Dog 1	185 mg IV (2)	12	34.8	PR	1	288	582
Dog 2	240 mg IL (2)	12	30.6 (175)	CR	4[a]	>560	>560
Cat 1	35 mg IL (2)[b]	12	38.3	CR	1	320	>500
Cat 2	50 mg IL (2)	12	36.0	PR	0	>330	>330

CEM43°C$_I$, cumulative equivalent minutes at 43°C invasive measurement; CEM43°C$_S$, cumulative equivalent minutes at 43°C surface measurement; CR, complete response; IL, intralesional; IV, intravenous; PR, partial response.
All response parameters refer to target lesions only. Horse 1 died of congestive heart failure at 430 days, cat 2 was lost to follow up at 330 days, while dog 1 and cat 1 developed progressive disease at 288 and 320 days, respectively. Additional combination therapy (hyperthermia and carboplatin) was pursued in dog 1 resulting in prolonged intervals of stable disease (224 days). Horse 2 and dog 2 show no evidence of local recurrence and remain tumour free.
[a]Patients that developed tumour necrosis.
[b]Dosage reduction (25%) because of pre-existing renal insufficiency.

dose (CEM43°C) averaged 160 and 175 min per treatment in these two patients. These values are compared to their average non-invasive thermal doses of 3.2 and 2.6 min per treatment as measured at the skin-antenna interface, respectively. Time to reach treatment temperatures of ≥39°C ranged from 6 to 15 min (mean = 9, median = 11) while time to reach maximum surface temperature of 41°C ranged from 8 to 23 min (mean = 13, median = 14).

Objective tumour responses were noted in all treated patients (Table 3). Time to response ranged from one week (horse 1) to eight weeks (horse 2 and dog 2) with an average of 4.8 weeks (median 4 weeks). A partial response was noted in one cat (cat 2) with a locally advanced fibrosarcoma and one dog with an extensive maxillary osteosarcoma (dog 1). Cat 2 had a 60% reduction in maximum tumour diameter while dog 2 had a 75% reduction in maximum tumour diameter (Fig. 6). Complete

responses were seen in the remaining four patients; although response evaluation was typically delayed (4 weeks) until after the resolution of acute side effects in these patients. Duration of initial local tumour control varied from 228 days to greater than 560 days; with one dog (dog 1) and the two cats exhibiting local tumour recurrence/progression as their first events.

Severe haematologic toxicity from therapy was noted in two patients and necessitated dosage reductions (20%) for subsequent chemotherapy treatments. Treatment-related local tissue toxicity was observed in five patients (Table 3). In two patients, the toxicity was severe (grade IV) and seen as early as 4 days (horse 1) and as late as 6 weeks (dog 2) after the initial treatment. Acute tumour necrosis occurred in horse 1 during the first week of therapy. No further treatments were pursued in this horse, tumour clearance occurred and no comprise in the healing of normal tissues or re-epithelialization was
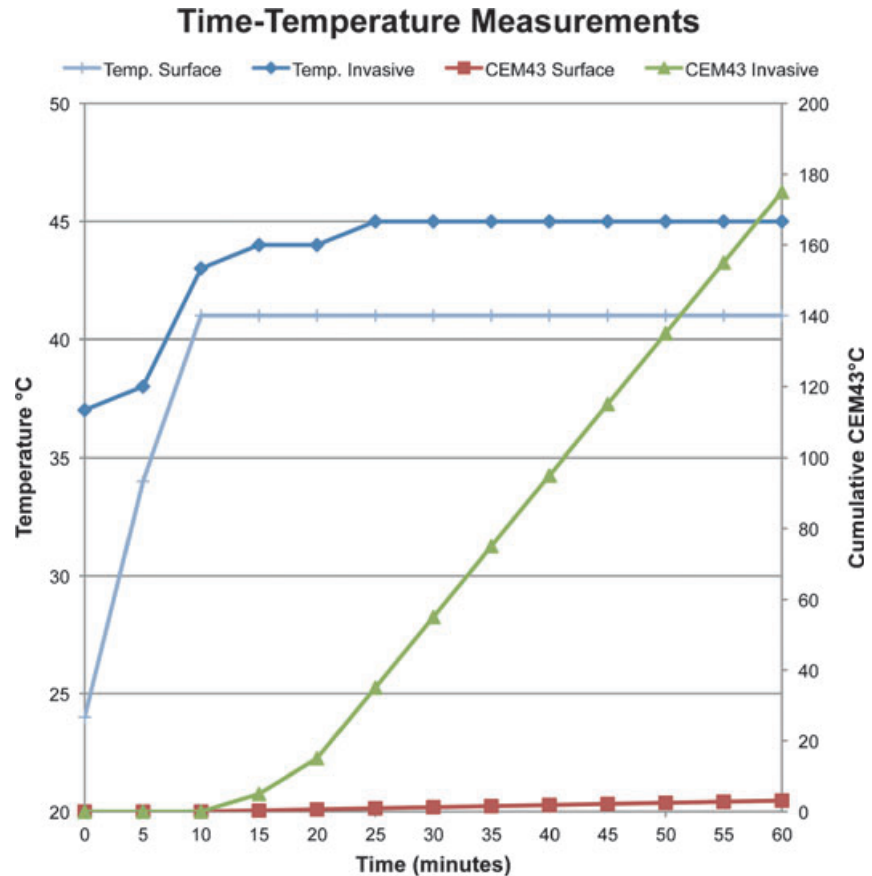
Figure 5. Time-temperature profile from a single 60-min treatment in dog 2. Actual temperature measurements are shown on the left axis, while cumulative equivalent minutes at 43°C (CEM43°C) are shown on the right axis. A thermal gradient of 3–4°C is seen between non-invasive and invasive temperature measurements resulting in a significant difference between CEM43°C as determined from non-invasive and invasive measurements. Therapeutic temperatures (>39°C) are achieved in less than 10 min as determined by surface and intra-tumoural measurements. Temperature surface = surface temperature measurements (±0.5°C); Temperature invasive = average intra-tumoural temperature measured along catheter track ~4-cm deep within tumour; CEM43 surface = cumulative equivalent minutes at 43°C as measured on the surface; CEM43 invasive = cumulative equivalent minutes at 43°C as measured intra-tumourally.

noted (Fig. 6). Tumour necrosis was also seen in dog 2, first noted 2 weeks after the completion of the prescribed thermal dose. Resolution of these side effects was delayed, ultimately requiring surgical closure, because of their local extent and the development of a secondary infection. Side effects had resolved completely by re-evaluation, 4 weeks after the completion of therapy. Finally, while no typical late toxicities were seen, dog 1 developed an oro-nasal fistula in place of the resolving tumour. Slight tumour re-growth allowed resolution of the fistula, resulting in a control period of 228 days. No further acute or late side effects were seen within the treatment field.

Discussion

Here, we describe simulation data and clinical use of a conformal ultra-wideband multilayer antenna for the delivery of therapeutic hyperthermia. Our simulation results illustrate a favourable electric field and power distribution compared to a similar dimension microstrip (flat) antenna. When compared to a flat antenna, the electric field exhibits a relative sparing of the near field skin-applicator interface along with improved energy transmission and depth of penetration. Directivity is further improved by the addition of a floating shield plane. This electric field pattern demonstrates the focusing ability of the antenna through its'

Figure 6. Clinical response seen in horse 1 (A−B) and dog 1 (C−D). (A) Pre-treatment images of a tail-base melanoma in a 21-year-old Paso Fino Stallion (arrow). (B) Post-treatment image (horse 1) following resolution of acute side effects, note the complete response. (C) Pre-treatment images of a maxillary osteosarcoma in a 6-year-old spayed female mixed breed dog (dog 1). (D) Post-treatment images of the same dog following 4 weeks of combination chemotherapy and hyperthermia; note the complete resolution of the external mass. Hyperpigmentation and alopecia is seen within the treatment field.

multilayer construct. A comparable flat antenna lacks this focusing ability and exhibits inferior energy transmission at 434 MHz as measured by return loss. The resultant increased voltage standing wave seen with a simple flat antenna would require the use of a water bolus to provide effective cooling of the skin surface and avoid superficial toxicity. Traditional microstrip and waveguide applicators for superficial hyperthermia also require the use of a water bolus for a variety of reasons including high return loss values.[5−7,14,39,32,33] The skin sparing effect of the multi-layer construct described herein requires no such water bolus for clinical use.

Simulation data was also used to estimate comparative EFS and EHD as measures of overall antenna efficiency.[27,39] EFS is defined as the ratio of the 50% SAR_{max} contour area to the physical area of the radiating aperture face. Older designs of microwave antennae utilize metal waveguides, which tend to produce a relatively small EFS. For example, the simulated EFS for a waveguide antenna with a 12.55 cm × 9.03 cm aperture is 27%.[39] Newer designs of microwave antennae have improved values for EFS; consider the commercially available dual-armed Archimedean spiral array applicator with an average EFS of 211% per antenna.[27] The EFS for the CUMLA is also quite favourable at 208%. Similarly, EHD is defined as the distance beyond 1 cm at which the SAR has decreased to 50% of the value seen at 1-cm depth.[7] The calculated EHD for a plane wave at 434 MHz frequency is 1.41 cm.[6] Both simulations

and phantom measurements have been performed on varying designs of microstrip applicators tuned to a frequency of 434 MHz. Reported values for the EHD from these measurements varies based on applicator design and boundary condition but has been reported at between 1.30 and 1.40 cm.[6,7,40] Simulations for the CUMLA suggest an EHD of 2.38 cm, which is superior to both the plane wave and comparable conformal antennae. Furthermore, the design characteristics of the CUMLA can be easily modified to allow for the creation of antennae arrays and alternate patch/slot structures to improve EFS and EHD to treat larger and/or deeper tumours, respectively.

Antenna efficiency was also evaluated through simulation of bandwidth and return loss. Bandwidth measures the breadth of resonance frequencies that result in efficient energy transfer ($S_{11} < -10$ dB) for a given antenna. Different anatomic sites have varying electrical properties, and thus resonant frequencies, based on tissue content.[26] Because of this, antennae with wideband properties over their working frequencies allow more flexibility in clinical use. Waveguide and many microstrip applicators have characteristically narrow bandwidths at centre frequencies of 434 MHz with typical values of 31–50 MHz.[26,39] Spiral microstrip antennae are inherently broad band; the bandwidth of the dual-arm Archimedean spiral array is 150 MHz at a centre frequency of 600 MHz.[27] However, at the working frequency of 915 MHz, the bandwidth of the spiral array is less than 50 MHz with an average return loss of −8.2 dB.[19] The CUMLA incorporates a slot-antenna and multi-layer construct to improve bandwidth performance.[14,32] Simulation results show a bandwidth of >350 MHz at a centre frequency of 434 MHz and were in general agreement with measured results (Fig. 4). The variation seen between the simulated and measured results was likely attributable to differences in boundary conditions in the simulation versus *in vivo*.

The clinical utility of the conformal antenna was evaluated in a small cohort of veterinary patients receiving carboplatin chemotherapy. A variety of species and tumour types were included to illustrate the broad applicability of this technology. Clinical responses were seen in all patients;

although treatment-limiting toxicity occurred in two patients. The tissue necrosis seen in horse 1 and dog 2 were full-thickness lesions that included the entire tumour along with margins of adjacent normal tissue. Determination of the exact mechanism of this toxicity requires an understanding of the thermal field created during treatments. On the basis of the patient (tumour location and patient tolerance) and technical constraints, we utilized a minimal approach to thermal assessment by placing thermometers at predicted locations of minimum (∼4 cm) and maximum (skin) electric field.[27] The thermometry methods used herein, however, were inadequate to define any existing field irregularities or resulting 'hot spots' in the treatment field. Specifically, 'hot spots' can be created at the interface of tissues with differing electrical properties. Muscle tissue has relative high electric conductivity and permittivity in comparison to the underlying bone tissue,[26] these differences can lead to accumulation of charge along the interface and resultant overheating. The thermal burns may also be because of electric field variations that occur when conforming the antenna around an extremity. In general, the behaviour of electromagnetic fields has been shown to vary between flat and curved configurations of conformal antennae.[33] Furthermore, we noted detectable changes in bandwidth between flat and curved configurations of the CUMLA (Table 1). In addition to the heterogeneity noted in electric field properties, perfusion-related conductive cooling that occurs in tissues also likely contributed to overall temperature heterogeneity and resultant difficulties in dosimetry.[41] While multiple invasive thermoprobes may have allowed improved accuracy in thermal dose prescription; deep thermal burns were still seen with a frequency up to 14%.[8] Larger clinical studies and more extensive thermal dose description are required to determine the mechanism underlying the thermal burns seen in this patient.

Clinical responses seen in this cohort of patients include two partial and four complete remissions. The patients with partial responses (dog 1 and cat 2) exhibited no treatment-related local tissue toxicities and had control periods of 228 and >330 days, respectively. Additional monthly treatments with hyperthermia and chemotherapy appeared necessary to maintain

stable disease in dog 1. Two of the patients with complete responses (horse 1 and dog 2) developed rapid tumour death consistent with thermal necrosis; although histologic assessment was not performed. While tumour necrosis can occur at lower temperatures, it becomes increasingly more common as temperature increases above 43°C.[36] The addition of chemotherapy in these patients would be expected to cause further tumour destruction (increased response rate); lowering the threshold for tumour necrosis.[24] In addition to a more extensive thermal dose description, evaluation of chemotherapy dosage and tumour histologic response may inform on the mechanism of toxicity seen in these patients. The remaining patients had gradual tumour reduction until a complete remission was achieved. While no local tumour recurrence was seen in either horse, cat 1 required intermittent chemotherapy and hyperthermia treatments for new and recurrent tumour re-growth.

In summary, we have provided simulation data to illustrate the favourable electrical field properties of the CUMLA in comparison to a simple flat antenna in soft tissue equivalent boundary conditions. Treatments delivered with this CUMLA, in conjunction with carboplatin chemotherapy, were found to have clinical activity in horses, dogs and cats with solid malignancies. This combination therapy documented objective responses in both locally advanced and refractory tumours; tumours that are often considered untreatable. Severe local tissue toxicity (Grade IV) was seen in two patients; requiring surgical closure in one patient. Further evaluation is needed to determine appropriate indications for this combination therapy and to optimize thermal dosimetry, specifically for extremity regions. Future goals include investigating the prospective activity of hyperthermia alone versus this combination therapy in companion animals, designing novel antennae for challenging anatomic locations, and optimizing treatment schedules.

References

1. Stauffer PR. Evolving technology for thermal therapy of cancer. *International Journal of Hyperthermia* 2005; **21**: 731–744.

2. Antonlini R, Cerri G, Cristoforetti L and De Leo R. Absorbed power distribution from single or multiple waveguide applicators during microwave hyperthermia. *Physics in Medicine and Biology* 1986; **31**: 1005–1019.

3. Sherar MD, Clark H, Cooper B, Kumaradas J and Liu FF. A variable microwave array attenuator for use with single-element waveguide applicators. *International Journal of Hyperthermia* 1994; **10**: 723–731.

4. Juang T, Neuman D, Schlorff J and Stauffer PR. Construction of a conformal water bolus west applicator for hyperthermia treatment of superficial skin cancer. *Conference Proceedings: IEEE Engineering in Medicine and Biological Society* 2004; **5**: 3467–3470.

5. Montecchia F. Microstrip-antenna design for hyperthermia treatment of superficial tumors. *IEEE Transactions on Bio-medical Engineering* 1992; **39**: 580–588.

6. Petra Kok H, De Greef M, Correia D *et al*. FDTD simulations to assess the performance of CFMA-434 applicators for superficial hyperthermia. *International Journal of Hyperthermia* 2009; **25**: 462–476.

7. Lamaitre G, Van Dijk JDP, Gelvich EA, Wiersma J and Schneider CJ. SAR characteristics of three types of flexible microstrip applicators for superficial hyperthermia. *International Journal of Hyperthermia* 1996; **12**: 255–269.

8. Thrall DE, LaRue SM, Yu D *et al*. Thermal dose is related to duration of local control in canine sarcomas treated with thermoradiotherapy. *Clinical Cancer Research* 2005; **11**: 5206–5214.

9. Kumaradas JC and Sherer MD. An edge-element based finite element model of microwave heating in hyperthermia: application to a bolus design. *International Journal of Hyperthermia* 2002; **18**: 441–453.

10. Ammann M, Curto S, Bao X and McEvoy P. Antenna design considerations for high specific absorption rate in local hyperthermia treatment, *IEEE International Symposium Antennas and Propagation Society*, San Diego, CA, 5–11 July 2008. 1–4

11. Veselago VG. Properties of materials having simultaneously negative values of the dielectric and magnetic susceptibilities. *Soviet Physics-Solid State* 1967; **8**: 2854–2856.

12. Liu Y and Zhang X. Metamaterials: a new frontier of science and technology. *Chemical Society Reviews* 2011; **40**: 2494–2507.

13. Enoch S, Tayeb G, Sabouroux P, Guerin N and Vincent P. A metamaterial for directive emission. *Physical Review Letters* 2002; **89**: 21–25.

14. Zhang H, Xin H, Bortolin R and Kudva J. A compact metamaterial-inspired multilayered slot antenna. *Microwave and Optical Technology Letters* 2011; **53**: 219–223.

15. Karathanasis KT, Karanasiou IS and Uzunoglu NK. Enhancing the focusing properties of a prototype non-invasive brain hyperthermia system: a simulation study. *Conference Proceedings: IEEE Engineering in Medicine and Biological Society* 2007 Lyon, France; 218–221.

16. Wang G and Gong Y. Metamaterial lens applicator for microwave hyperthermia of breast cancer. *International Journal of Hyperthermia* 2009; **25**: 434–445.

17. Dewhirst MW and Sims DA. The utility of thermal dose as a predictor of tumor and normal tissue responses to combined radiation and hyperthermia. *Cancer Research* 1984; **44**: 4772s–4780s.

18. Gillette EL. Large animal studies of hyperthermia and irradiation. *Cancer Research* 1979; **39**: 2242–2244.

19. Theon AP, Madewell BR, Moore AS, Stephens C and Krag DN. Localized thermo-cisplatin therapy: a pilot-study in spontaneous canine and feline tumours. *International Journal of Hyperthermia* 1991; **7**: 881–892.

20. Page RL, Thrall DE, George SL *et al*. Quantitative estimation of the thermal dose-modifying factor for cis-diamminedichloroplatinum in tumour-bearing dogs. *International Journal of Hyperthermia* 1992; **8**: 761–769.

21. Urano M, Kuroda M and Nishimura Y. For the clinical application of thermochemotherapy given at mild temperatures. *International Journal of Hyperthermia* 1999; **15**: 79–107.

22. Dahl O. Interaction of heat and drugs in vitro and in vivo. In: *Thermoradiotherapy and Thermochemotherapy*, MH Seegenschmiedt, P Fessenden and CC Vernon, eds., vol 1, Berlin, Springer, 1995: 103–121.

23. Linder LH and Issels RD. Hyperthermia in soft tissue sarcoma. *Current Treatment Options in Oncology* 2011; **12**: 12–20.

24. Issels RD. Hyperthermia and thermochemotherapy. *Cancer Treatment and Research* 1993; **67**: 143–160.

25. Paulsen KD, Jia X and Sullivan JM Jr. Finite element computations of specific absorption rates in anatomically conforming full-body models for hyperthermia treatment analysis. *IEEE Transactions on Bio-medical Engineering* 1993; **40**: 933–945.

26. Gabriel S, Lau RW and Gabriel C. The dielectric properties of biological tissues: II. Measurements in the frequency range 10 Hz to 20 GHz. *Physics in Medicine and Biology* 1996; **41**: 2251–2269.

27. Johnson JE, Neuman DG, Maccarini PF, Juang T, Stauffer PR and Turner P. Evaluation of dual-arm Archimedean spiral array for microwave hyperthermia. *International Journal of Hyperthermia* 2006; **6**: 475–490.

28. Owen LN. *TNM Classification of Tumors in Domestic Animals.*, Geneva, World Health Organization.

29. Page RL, McEntee MC, George SL *et al*. Pharmacokinetic and phase I evaluation of carboplatin in dogs. *Journal of Veterinary Internal Medicine* 1993; **7**: 235–240.

30. Kisseberth WC, Vail DM, Yaissle J *et al*. Phase I clinical evaluation of carboplatin in tumor-bearing cats: a Veterinary Cooperative Oncology Group study. *Journal of Veterinary Internal Medicine* 2008; **22**: 83–88.

31. Théon AP, Wilson WD, Magdesian KG, Pusterla N, Snyder JR and Galuppo LD. Long-term outcome associated with intratumoral chemotherapy with cisplatin for cutaneous tumors in equidae: 573 cases (1995-2004). *Journal of the American Veterinary Medical Association* 2007; **230**: 1506–1513.

32. Drizdal T, Vrba M, Cifra M, Togni P and Vrba J. Feasibility study of superficial hyperthermia treatment planning using COMSOL multiphysics. *IEEE Proceedings of the 14th Conference on Microwave Techniques* 2008 Prague, Czeck Republic; 155–158.

33. Correia D, Kok HP, de Greef M, Bel A, van Wieringen N and Crezee J. Body conformal antennas for superficial hyperthermia: the impact of bending contact flexible microstrip applicators on the electromagnetic behavior. *IEEE Transactions on Bio-medical Engineering* 2009; **56**: 2917–2926.

34. Nussbaum G. Quality assessment and assurance in clinical hyperthermia: requirements and procedures. *Cancer Research* 1984; **44**(Suppl. 10): 4811s–4817s.

35. Myerson RJ, Straube WL, Moros EG *et al*. Simultaneous superficial hyperthermia and external radiotherapy: report of thermal dosimetry and tolerance to treatment. *International Journal of Hyperthermia* 1999; **15**: 251–266.

36. Sapareto SA and Dewey WC. Thermal dose determination in cancer therapy. *International Journal of Radiation Oncology, Biology, Physics* 1984; **10**: 787–800.

37. Eisenhauer EA, Therasse P, Bogaerts J *et al*. New response evaluation criteria in solid tumours:

revised RECIST guideline (version 1.1). *European Journal of Cancer* 2009; **45**: 228–247.

38. Veterinary Co-operative Oncology Group (VCOG). Veterinary Co-operative Oncology Group – Common Terminology for Adverse Events (VCOG-CTCAE) following chemotherapy or biological antineoplastic therapy in dogs and cats v1.0. *Veterinary and Comparative Oncology* 2004; **2**: 195–213.

39. Ebrahimi-Ganjeh MA. Study of water bolus effect on SAR penetration depth and effective field size for local hyperthermia. *Progress in Electromagnetics Research B* 2008; **4**: 273–283.

40. van Wieringen N, Wiersma J, Zum Vorde Sive Vording P *et al*. Characteristics and performance evaluation of the capacitive Contact Flexible Microstrip Applicator operating at 70 MHz for external hyperthermia. *International Journal of Hyperthermia* 2009; **25**: 542–553.

41. Chen Z and Roemer R. The effects of large blood vessels, on temperature distributions during simulated hyperthermia. *Journal of Biomechanical Engineering* 1992; **114**: 473–481.